Lawrence Berkeley National Laboratory

Title

Chemical changes in thirdhand smoke associated with remediation using an ozone generator

Permalink

https://escholarship.org/uc/item/27q5v94j

Authors

Tang, Xiaochen
González, Noelia Ramírez
Russell, Marion L
et al.

Peer reviewed

Chemical changes in thirdhand smoke associated with remediation using an ozone generator

Xiaochen Tang[a,*], Noelia Ramirez Gonzalez[b,c], Marion L. Russell[a],
Randy L. Maddalena[a], Lara A. Gundel[a], Hugo Destaillats[a,*]

[a] Indoor Environment Group, Lawrence Berkeley National Laboratory,
Berkeley, California, USA

[b] Institut d'Investigació Sanitària Pere Virgili, Tarragona, Spain

[c] Universitat Rovira i Virgili, Department of Electronic Engineering,
MIL@b, CIBERDEM, Tarragona, Spain

[*]*Corresponding authors*

Email: XTang@lbl.gov, HDestaillats@lbl.gov

Mailing Address: 1 Cyclotron Rd, M/S 70R0108B, Berkeley, CA 94720

Abstract

Ozonation is a common remediation approach to eliminate odors from mold, tobacco and fire damage in buildings. Little information exists to: 1) assess its effectiveness; 2) provide guidance on operation conditions; and 3) identify potential risks associated with the presence of indoor ozone and ozonation byproducts. The goal of this study is to evaluate chemical changes in thirdhand smoke (THS) aerosols induced by high levels of ozone, in comparison with THS aerosols aged under similar conditions in the absence of ozone. Samples representing different stages of smoke aging in the absence of ozone, including freshly emitted secondhand smoke (SHS) and THS, were collected inside an 18-m^3 room-sized chamber over a period of 42 hours after six cigarettes were consumed. The experiments involved collection and analysis of gas phase species including volatile organic compounds (VOCs), volatile carbonyls, semivolatile organic compounds (SVOCs), and particulate matter. VOC analysis was carried out by gas chromatography/mass spectrometry with a thermal desorption inlet (TD-GC/MS), and volatile carbonyls were analyzed by on-line derivatization with dinitrophenylhydrazine (DNPH), followed by liquid chromatography with UV/VIS detection. SVOCs were extracted from XAD-coated denuders and Teflon-coated fiberglass filters in the absence of ozone. In those extracts, tobacco-specific nitrosamines (TSNAs) and other SVOCs were analyzed by gas chromatography with positive chemical ionization-triple quadrupole mass spectrometric detection (GC/PCI-QQQ-MS), and polycyclic aromatic hydrocarbons (PAHs) were quantified by gas chromatography with ion trap mass spectrometric detection (GC/IT-MS) in selected ion monitoring mode. Particulate matter concentration was determined gravimetrically. In a second experiment, a 300 mg h^{-1} commercial ozone generator was operated during one hour, one day after smoke was generated, to evaluate the remediation of THS by ozonation. VOCs and volatile carbonyls were analyzed before and after ozonation. Extracts from fabrics that were exposed in the chamber before and after ozonation as surrogates for indoor furnishings were analyzed by GC/IT-MS, and aerosol size distribution was studied with a real-time scanning mobility particle sizer. Ozone concentration was measured with a photometric detector. An estimated 175 mg ozone reacted with THS after one hour of treatment, corresponding to 58% of the total O_3 released during that period. Fabric-bound nicotine was depleted after ozonation, and the surface concentration of PAHs adsorbed to fabric specimens decreased by an order of magnitude due to reaction with ozone, reaching pre-smoking levels. These results suggest that ozonation has the potential to remove harmful THS chemicals from indoor surfaces. However, gas phase concentrations of volatile carbonyls, including formaldehyde, acetaldehyde and acetone were higher immediately after ozonation. Ultrafine particles (UFP, in most cases with size <60 nm) were a major ozonation byproduct. UFP number concentrations peaked shortly after ozonation ended, and remained at higher-than background levels for several hours. Based on these results, minimum re-entry times after ozone treatment were predicted for different indoor scenarios. Clearly defining re-

entry times can serve as a practical measure to prevent acute human exposure to ozone and harmful ozonation byproducts after treatment. This study evaluated potential benefits and risks associated with THS remediation using ozone, providing insights into this technology.

1. Introduction

The publication of the 1986 US Surgeon General's Report on the health effects of exposure to secondhand tobacco smoke (SHS) led to widespread recognition of the need for protection of non-smokers (Koop 1986). Twenty years later, a second Surgeon General's Report updated the evidence of the harmful effects associated with SHS exposures, and identified critical gaps in the knowledge base for characterizing SHS, assessing exposure to non-smokers, and understanding related health effects (U.S. Department of Health and Human Services 2006) . During the last three decades, evidence of the dynamic behavior of SHS indoors has accumulated, illustrating the persistence of tobacco-related pollutants long after smoking ends. More recently, the term *thirdhand smoke* (THS) was introduced to differentiate direct (secondhand) exposures to smoke from indirect exposures commonly found in indoor environments. THS comprises chemical residues left behind by tobacco smoking, resulting in long-term, and often surface-mediated, exposures (Matt et al. 2011, Jacob et al. 2017). THS is different from freshly emitted SHS in its chemical composition, indoor residence time, and exposure pathways. THS constituents absorb into materials, settle onto surfaces and dust, and can be re-emitted and/or resuspended into indoor air long after smoking ends (Destaillats et al. 2006, Hoh et al. 2012, Bahl et al. 2014, Sleiman et al. 2014, Matt et al. 2017, Collins et al. 2018, DeCarlo et al. 2018, Matt et al. 2018, Sheu et al. 2020). This dynamic system produces complex contaminant mixtures that include both persistent smoke constituents and byproducts of indoor chemical transformations. For example, nicotine reacts with indoor ozone to generate ultrafine particles and irritating compounds (Destaillats et al. 2006, Sleiman et al. 2010a). Reaction of nicotine with hydroxyl radicals yields formamide and isocyanic acid (Borduas et al. 2016), and its reaction with nitrous acid (HONO) yields carcinogenic tobacco-specific nitrosamines (TSNAs) (Sleiman et al. 2010b).

Building occupants can be exposed to THS through different pathways: inhalation, dermal uptake, and (particularly in the case of infants and toddlers) the mouthing of contaminated objects. Because of the persistence of THS, such exposures can take place hours, days or weeks after smoking has ended, potentially leading to unexpected adverse health effects. With the successful implementation of policies restricting smoking in public places, the home has become the main setting for non-smokers' exposures. If smokers actively avoid consuming cigarettes in the presence of other members of their household (often children), these non-smokers may be mostly exposed to THS, rather than SHS. Our previous study

has assessed the potential exposure risk and impact of the inhalable particles and gases on human health by computing the associated loss of disability-adjusted life years (DALYs), and found that exposure to THS can account for 5−60% of the total harm caused by exposure to tobacco-related pollutants in SHS and THS indoors, which is estimated to be 0.7−1.1 life years over 50 years of living with a smoker who consumes 28 cigarettes per day (Sleiman et al. 2014). As more evidence of the negative impacts of THS emerges, there is a growing need to better understand the potential benefits and risks of different THS remediation approaches, including ozonation.

Ozone is the main atmospheric oxidant driving indoor chemistry. It reacts with unsaturated organic compounds in indoor air, surface-bound chemicals, and material surfaces (Weschler 2000, Morrison and Nazaroff 2002, Singer et al. 2006, Wang and Morrison 2006, Weschler 2006, Wisthaler and Weschler 2010). Ultrafine particles, volatile aldehydes and other harmful volatile organic compounds (VOCs) have been reported as the main byproducts (Fan et al. 2003, Sarwar et al. 2003, Nazaroff and Weschler 2004, Hubbard et al. 2005, Destaillats et al. 2006, Coleman et al. 2008, Rim et al. 2016). This chemistry can be initiated by the relatively low ozone levels commonly found indoors due to infiltration from polluted outdoor air, often below 20 ppb (Zhang and Lioy 1994, Weschler 2000, Stephens et al. 2012, Weschler and Carslaw 2018). In some cases, ozone can also be generated from indoor sources such as home appliances (Zhang and Jenkins 2017) and office equipment, e.g. copiers and laser printers (Destaillats et al. 2008, Wang et al. 2012, Guo et al. 2019). Ozone can be emitted by air cleaners as a byproduct, for example in ion generators (Niu et al. 2001, Tung et al. 2005, Britigan et al. 2006, Waring and Siegel 2011), or can be produced intentionally at very high levels, up to several hundreds of ppb (Tung et al. 2005, Britigan et al. 2006, Poppendieck et al. 2014). The latter are marketed as "air purifiers" removing indoor allergens, odorous compounds, mold, viruses, and bacteria, and their use is discouraged by the California Air Resources Board (CARB 2020) and other organizations. Even stronger ozone generators are used in the restoration of buildings that have been damaged by flood, mold or fire, and to treat offensive odors (Serra et al. 2003, Brodowska et al. 2018). Operation of these devices, which often deliver between hundreds of mg and up to 10 g of ozone per hour, is specified for unoccupied spaces to prevent acute occupant exposures to high ozone levels, which may reach from several hundreds to thousands of ppb. Little attention has been paid to effects associated with operation of these devices in the remediation of THS, and the related occupant exposures after treatment.

This study investigated changes taking place in THS aerosol composition as it aged during 42 hours after smoking, and the effect of ozonation by operating a commercial generator commonly used to remove THS odors. Key tobacco-related contaminants, including volatile carbonyls, nitrogenated compounds and polycyclic aromatic hydrocarbons (PAHs), were identified and quantified as a function of aging time,

along with the concentration of particulate matter. The objective of the study was to identify benefits and explore potential problems associated with THS remediation using ozonation. Determining the appropriate air exchange rate and minimum re-entry time required after treatment is needed to minimize exposures to hazardous airborne ozonation byproducts.

2. Experimental Methods

Table S1 (Supporting Information) describes the two experiments carried out to assess THS aerosol aging and the effects of ozonation on aged THS, respectively. In the first one, THS was aged without adding ozone, and in the second experiment (THS+O_3), ozonation was carried out by operating a commercial ozone generator several hours after smoking ended. In both experiments, six cigarettes were smoldered simultaneously to generate fresh SHS inside the chamber under similar conditions. Samples of gas phase species and airborne particulate matter (PM) were collected prior to and after smoking, over a 2-day period. Table S1 shows the start time and duration of each sample. The time scale considers the end of the smoking event as t = 0 h, with the time prior to smoking represented with negative values. During the month elapsed between the two tests, the chamber was naturally ventilated with the door open. Before the start of the THS+O_3 experiment, sections of three fabrics (cotton, wool, polyester), with total surface area of 12 m^2 were hung inside the chamber to study the effects of ozonation on THS contaminants present on the surface of furnishings. To examine the influence of elevated O_3 concentration on background air and surface components before generating THS, the ozone generator was operated for one hour prior to smoking. All other experimental conditions were similar to those of the THS aging experiment. Chamber ozone concentration was monitored continuously, as well as the fine particle number concentration and size distribution. Swatches of the fabrics were collected at different stages of the experiment, extracted and analyzed for adsorbed THS constituents.

2.1 Environmental chamber

Experiments were carried out in an 18 m^3 room-sized chamber at Lawrence Berkeley National Laboratory (LBNL), configured as illustrated in Figure S1 (Supporting Information). The walls and ceiling of the chamber were built with painted gypsum wallboard (42 m^2), and the floor (10 m^2) was covered with vinyl tiles. Neither the walls had been repainted, nor had the floor tiles been replaced for at least 8 years; hence, no major VOC contributions from those materials were expected. The chamber had one door, several sampling ports that were not tightly sealed, and a vent covered with a pleated air filter in the middle of the ceiling. Two standing fans in the chamber ensured rapid mixing during the experiments. The air exchange rate (*AER*) was calculated by following the concentrations of CO_2 generated during the smoking phase. A

rapid pulse of CO_2 was introduced into the chamber to reach an initial concentration of ca. 2,500 ppm, which was significantly higher than ambient levels. Real time CO_2 concentration decay was monitored and recorded with a CO_2 sensor, until CO_2 levels dropped close to ambient levels (~410 ppm). After subtracting the measured ambient CO_2 level, the curves of CO_2 concentration vs. time were fitted with mono-exponential decay functions. The resulting *AER* values were 0.30 h^{-1} during the THS aging experiment, and 0.17 h^{-1} during the THS ozonation experiment. The air exchange was attributed to air sampling and leakage of outdoor air into the chamber. The difference between the two experiments is due to different airflow requirements of the various sampling methods used in each case. Immediately prior to each experiment, the chamber was fully ventilated using a high flow duct fan, with the door closed, to complete at least thirty air exchanges. Chamber background samples (chamber blank) were taken after the chamber was ventilated, and prior to the smoking phase.

2.2 Generation and aging of tobacco smoke in the laboratory

In each experiment, six cigarettes were lit and smoldered simultaneously until the tobacco was completely consumed. Cigarettes were purchased from local retailers in Berkeley, CA, immediately prior to the experiments. The cigarette brands were the same as those used in our previous study of THS VOC constituents (Sleiman et al. 2014): Camel 99s Turkish Domestic Blend (3 cigarettes) and Marlboro Special Blend (Smooth Mellow Flavor, 3 cigarettes). After smoking, the fresh cigarette smoke was allowed to age in the chamber as described in Table S1 (Supporting Information). In the "THS aging" experiment, the following samples were defined: freshly emitted smoke (*SHS*), the mixture of SHS and THS (*SHS/THS transition*), and two THS samples, defined as *THS*, and *aged THS (> 24h)*. As the experiment proceeded the sampling duration increased, in order to collect enough mass for analysis from the diluted indoor air resulting from continuous air exchange and loss to surfaces. In the THS ozonation experiment, conditions replicated those of the initial stages of the THS aging experiment. THS was sampled from 14 h to 16.3 h after smoking, overlapping with the beginning of the 14-h THS sample in the THS aging experiment. At t= 17.2 h, the 1-h ozone generation was started. The sample "THS post ozonation" was taken after indoor ozone concentration dropped below 30 ppb, and lasted for 2.1 h.

2.3 O_3 generation and monitoring

In the THS+O_3 experiment, a commercial corona discharge O_3 generator (Model QT Thunder QTT3F, Queenaire Technologies, Ogdensburg, NY) was used inside the chamber to produce O_3 continuously for one hour during three periods: to pre-quench chamber surfaces, immediately before smoking, and after the cigarette smoke aged for almost 20 hours, respectively. The O_3 generator was set to its maximum output (300 mg h^{-1}) and ran for 60 min (maximum timer setting). Indoor O_3 concentration was measured continuously using a photometric ozone monitor (Model 205, 2B Technologies, Colorado, US).

2.4 THS aerosol sampling

In both experiments, two 47-mm open-face aluminum filter holders were used in parallel to collect PM and determine the PM mass concentration gravimetrically. Air was drawn through two Teflon-coated glass fiber filters (Fiberfilm, T60A20, Pall Corp., Port Washington, NY) in series. The flow rate was 16.7 L min^{-1} for each of the filter holders, and the duration was recorded for each sample. PM sampling periods are shown in Table S1. Before use, the Teflon-coated glass fiber filters were pre-cleaned by soaking them in high purity (LC/pesticide analysis grade) ethyl acetate, followed by sonication for 30 minutes, then dried and stored in sealed glass containers. Before and after collecting particles, filters were conditioned in a temperature and humidity-controlled chamber, and weighed using a microbalance (Sartorius SE-2F, Goettingen, Germany, readability of 0.1 µg). The total PM mass concentration for each sampling period was determined as the sum of the aerosol mass on the upstream and downstream filters divided by the air sample volume.

In the THS aging experiment only, an Integrated Organic Gas and Particle Sampler (IOGAPS,(Gundel et al. 1995, Swartz et al. 2003) was used to simultaneously adsorb semivolatile gases on denuders and collect the denuded particles on filters. These additional samples enabled further characterization of the composition of both gases and particles as the THS aerosols aged. A cyclone inlet removed particles larger than 2.5 µm diameter, allowing gases and respirable particles (PM$_{2.5}$) to pass through an XAD-4-coated annular denuder (eight-channel, 52 mm OD; 30 cm length) that collected semi-volatile organic gases. PM$_{2.5}$ was collected downstream on a 90-mm diameter pre-weighed Teflon-coated glass fiber filter (Pallflex Emfab®, Pall Corporation, Ann Arbor, MI) followed by an XAD-4-coated quartz filter used as a backup trap for any remaining semivolatile organic compounds (SVOCs) in the gas stream, as well as SVOCs that desorbed from the first filter during sampling. The flow rate of the IOGAPS was 100 ± 5 L min^{-1}.

The Emfab filters used in the IOGAPS were pre-cleaned with ethyl acetate with the same protocol used for the 47-mm filters, conditioned and weighed on the microbalance before and after exposure to the air in the experimental chamber. PM collected on 90-mm Emfab filters corresponded to the mass of PM$_{2.5}$, while total PM in each stage was measured with the 47-mm Fiberfilm filters. After sampling and weighing, each of the Emfab Teflon-coated fiber glass filters were cut into four equally sized pieces, from which two were stored in a -20 °C freezer and two were extracted to characterize SVOC composition in the smoke samples, as described below.

After sampling, the XAD-4 coated denuders were spiked with an internal standard mixture (phenanthrene-d10 and flouranthrene-d10), before being extracted individually with ethyl acetate, to correct for any losses during sample preparation. The annuli in the denuder section were filled with about

30 ml of the extraction solvent. The extraction technique is discussed elsewhere (Gundel et al., 1995). Each extract was passed through a 47 mm diameter, 0.45 µm pore size Teflon filter (unlaminated, FHUP047, Millipore Corp.). The extract volumes were reduced to 5 mL using a TurboVap II system (Caliper Life Sciences) at 55 °C, then to a final volume of approximately 1 mL. Two unexposed coated denuders and clean filters were analyzed as blanks for every field test.

The Emfab filter pieces were extracted individually in ethyl acetate and processed in a similar way as the extracts of the denuders. Samples were put into separate glass vials, then spiked with a known amount of deuterated PAH internal standards, before adding 30 ml ethyl acetate. Soaked filter pieces were sonicated for 45 minutes to produce the first batch of extract solutions, which were transferred to another clean container. For a second extraction, another 30 ml ethyl acetate was added to the vial containing the filter piece, followed by 15-min sonication. The two extracts were combined before being filtered, and reduced to a smaller volume of ~ 1 ml, following the same method as that for the denuder extracts. Concentrated sample extracts from denuders and filters were stored in the freezer at -20 °C.

In the THS+O_3 experiment, particle size distribution and concentration were measured using a Scanning Mobility Particle Sizer (SMPS, Model 3936, TSI, Shoreview, MN) coupled with a water-based Condensational Particle Counter (CPC, Model 3781, TSI, Shoreview, MN). Particles in the size range of 10-400 nm diameter were monitored before and after the addition of O_3 to the chamber.

2.5 Chemical characterization of cigarette smoke

2.5.1 VOCs and carbonyls in chamber air samples

VOCs present in the smoke were sampled using multi-bed Carbopack sorbent tubes (Carbopack B and X, Supelco Inc, Bellefonte, PA). Air was pulled through two parallel sorbent tubes using peristaltic pumps, collecting duplicate samples in each sampling period. Identification and quantification of each compound was carried out by thermal desorption gas chromatography mass spectrometry (TD-GC/MS) using bromofluorobenzene as an internal standard (EPA 1984). An Agilent GC/MS system (model 6890/5973, CA, USA) was operated in electron impact mode and was interfaced with a thermal desorption inlet with an autosampler (Gerstel, Germany). Calibration curves were created for all VOCs for which authentic standards were available. Total VOC (TVOC) mass concentration was estimated by summing the peak areas of all detected compounds and calculated using the response factor of toluene, leading to the toluene-equivalent TVOC mass concentration.

Volatile carbonyls present in the chamber air were collected by using 2,4-dinitrophenylhydrazine (DNPH)-impregnated silica gel cartridges (Waters Corp., MA, USA). Air was pulled through the DNPH cartridges with a peristaltic pump, and duplicate samples were collected during each sampling period. The

cartridges were extracted with 2 mL of acetonitrile (carbonyl-free grade, Honeywell) and analyzed by high performance liquid chromatography (HPLC) with UV detection (Agilent 1200, CA, USA), following the EPA TO-11 method (EPA 1999). A certified mixture of DNPH derivatives was obtained from Sigma-Aldrich as standards for analysis of formaldehyde, acetaldehyde, acrolein, acetone, propanal, crotonaldehyde, methacrolein, butanal, methyl ethyl ketone, benzaldehyde, *m*-tolualdehyde and hexaldehyde.

2.5.2 Tobacco-specific semivolatile compounds in denuder and filter extracts

Denuder and filter extracts from the THS aging experiment were shipped (in dry ice) to Universitat Rovira i Virgili (Spain) for the analysis of TSNAs and other tobacco-related compounds by gas chromatography coupled with triple quadrupole mass spectrometry in positive chemical ionization mode (GC/PCI-QQQ-MS). The chromatographic system consisted on a 7890A GC system coupled to a 7000 QQQ MS (Agilent, CA, USA). Extracts were injected (1 μL) in a split/splitless inlet at 200 °C in pulsed splitless mode (30 psi for 2 min) and separated with a mid-polarity phase capillary column (35% diphenyl/65% polydimethylsiloxane, Zebron ZB-35, 30 m × 250 μm × 0.25 μm, from Phenomenex, Torrance, CA, USA) at a constant helium flow of 1.2 mL/min. Oven temperature was programmed at 100 °C for 1 min, increased at 25 °C min^{-1} to 225 °C, next at 5 °C min^{-1} to 240 °C and held at that temperature for 1 min.   Ionization was performed by positive chemical ionization using isobutene as reagent gas. Mass spectral data were acquired in multiple reaction monitoring mode with collision energy values optimized for each transition. Transfer line temperature and CI source were set at 250 °C. Quantification was performed by external standard calibration using isotope labelled standards of each target compounds.

2.5.3 PAHs on denuder, filter and fabric extracts

The denuder and filter extracts described above (in ethyl acetate) were also analyzed for PAHs by gas chromatography coupled with ion trap mass spectrometry (GC/IT-MS, Varian 4000, CA, USA) in selected ion monitoring (SIM) mode, using a mixture of 10 PAHs as quantification standards (EPA 8310 Mix, Supelco, USA). For the fabric samples, specimens were cut from the unexposed (control) and THS-impregnated fabric furnishings in the ozonation experiment. After collection, the swatches were weighed with the microbalance, then stored into amber vials. Specimens were pre-spiked with a known amount of internal standards (anthracene-d10, pyrene-d10, and benzo(a)pyrene-d12) to assess recovery efficiency. Extraction efficiency of spiked standards was evaluated with different solvents, from which dichloromethane (DCM) achieved the best performance. For that reason, extraction was carried out using two identical 15 mL DCM aliquots sequentially, with the first and second extracts analyzed separately in

order to evaluate extraction efficiency. Duplicate DCM extracts were analyzed by GC/IT-MS in SIM mode, using the same method as the denuder and filter extracts.

3. Results and discussion

3.1 Evolution of total VOC (TVOC), volatile carbonyls, and PM

Results corresponding to total VOCs (TVOC), volatile aldehydes and total PM concentration over the course of both experiments (THS aging and THS+O₃) are summarized in Figure 1. The background TVOC concentration at the beginning of the THS aging experiment was 16 μg m^{-3} (Figure 1-A). The TVOC concentration measured in fresh SHS immediately after smoking was 2,320 μg m^{-3}, representing approximately a ×150 factor increase. TVOC concentration slowly decayed over time due to ventilation, reaction and deposition onto indoor surfaces. The dashed lines shown in in Figure 1-A correspond to predicted TVOC concentration if these indoor contaminants were only removed by ventilation, in the absence of other loss pathways. The different slope for the predicted values in the THS aging and THS+O₃ experiments are due to the different *AER* in each experiment (0.30 and 0.17 h^{-1}, respectively). Average TVOC concentration in THS was higher than that estimated for ideal ventilation removal, suggesting that a fraction of VOCs that initially adsorbed onto indoor surfaces was desorbing back into the gas phase for several hours after smoking ended. THS aged overnight beyond the initial 24 hours contained 80 μg m^{-3} of TVOC, significantly higher than the estimated TVOC concentration in the absence of partitioning to indoor materials. Without sorptive losses and re-emission, TVOC would have dropped below 1 μg m^{-3} after 20 h. Remaining TVOC levels were much higher than the chamber background prior to smoking. This behavior is consistent with prior research carried out with tobacco smoke and other VOCs released in comparable environmental chambers (Singer et al. 2004). The identity and concentration of tobacco VOCs found in THS samples is provided in Table S2 (Supporting Information). Note that TVOC reported in Table S2 corresponds to the toluene-equivalent mass concentration of all VOCs measured in chamber air with TD-GC/MS, and not to the sum of individual VOCs listed in that table.

In the THS+O₃ experiment, background TVOC levels were 68 μg m^{-3}, approximately four times higher than in the THS aging tests. Compounds adsorbed to indoor structures and materials during the initial THS aging test remained as a long-term indoor emission source, despite additional ventilation at the end of the experiment and continuous partitioning with room air during the one-month interval between the two tests. Adding model furnishings served as a new sink for re-emitted contaminants, leading to a slight decrease of room air TVOC concentration to 54 μg m^{-3}. After ozone was introduced to the chamber with

furnishings, an increase of ~100 μg m^{-3} TVOC was observed, due to the formation of volatile byproducts of ozone-initiated indoor chemistry. The THS sample was taken at 14-16.3 hours after smoking took place. This sample had similar TVOC levels as in the THS aging experiment, 225 μg m^{-3}, slightly higher than the estimated ventilation removal level. After the 1-hr introduction of O$_3$, TVOC concentration increased to 354 μg m^{-3}, indicating formation of secondary organic compounds in the gaseous phase.
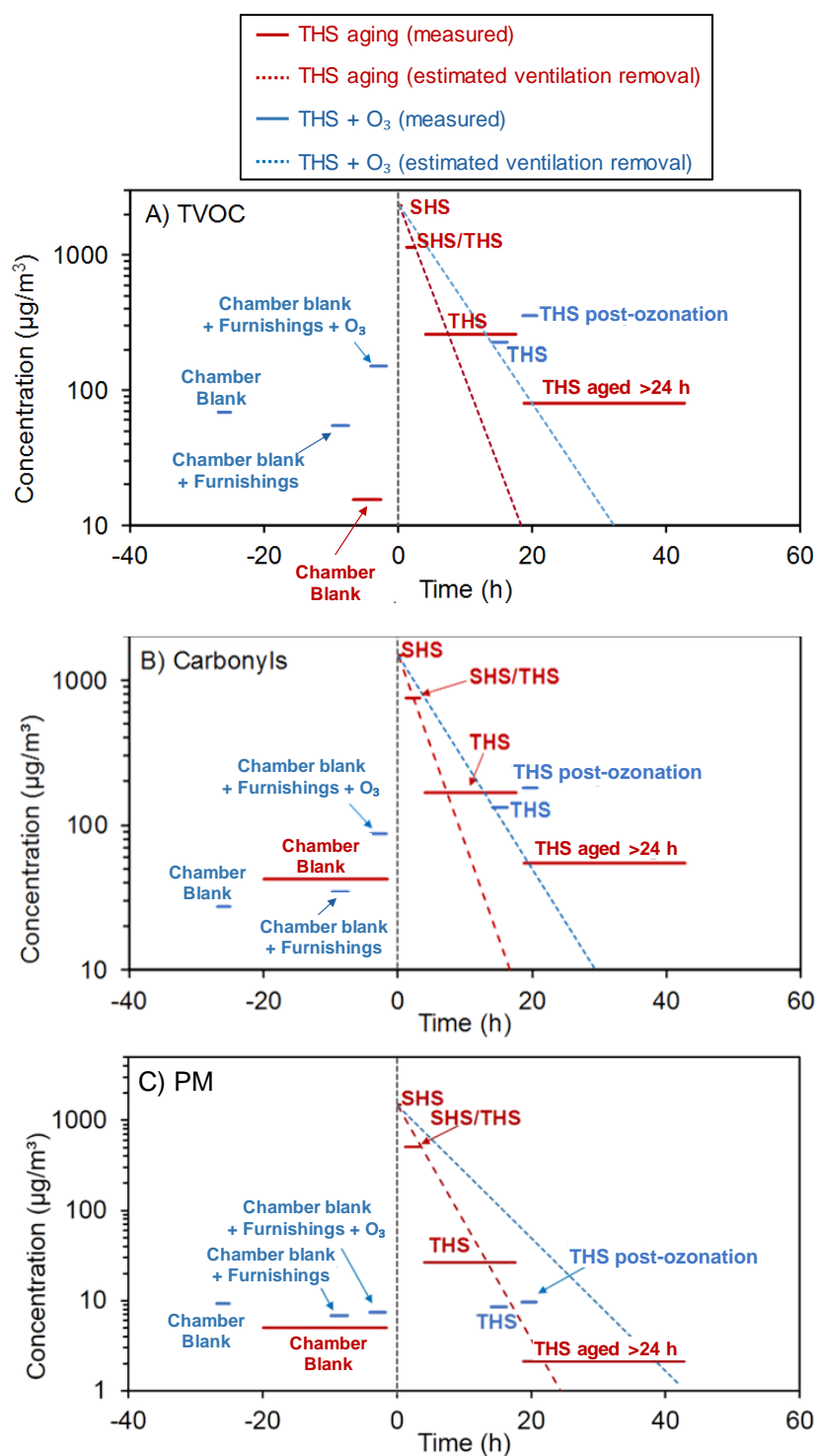
Figure 1: Average concentration in THS aging (red) and THS+O$_3$ (blue) experiment of (A) total VOC (TVOC), (B) volatile carbonyls, and (C) total PM mass.

The total concentration of 13 carbonyl compounds was determined in both experiments (Figure 1-B), showing similar trends as those described for TVOC. The identity and concentration of the most prevalent carbonyls found in THS are shown in Figure S2 and Table S3 (both in the Supporting Information). Among the measured carbonyl compounds, acetaldehyde, formaldehyde and acetone were the most abundant ones in the cigarette smoke. Background concentrations of other carbonyl were between 0.13 and 2.5 μg m^{-3}, while those of formaldehyde, acetaldehyde and acetone were between 8.3 and 14 μg m^{-3} (Table S3). In the THS aging experiment, indoor carbonyl levels spiked in fresh SHS, then quickly decayed in the first ~24 hours. All thirteen carbonyls were still present in the chamber air at least 24 h after smoking, with concentrations above 0.1 μg m^{-3}. The total concentration of remaining carbonyls found in the sample aged beyond the first day was 54 μg m^{-3}, comparable with the initial chamber blank (42 μg m^{-3}).

At least three compounds in THS exceeded established reference exposure levels (RELs), including acrolein (decreasing from 3.2 to 0.16 μg m^{-3}), methacrolein (from 5.6 to 1.0 μg m^{-3}), and acrylonitrile (from 6.8 μg m^{-3} to below DL). The California Office of Environmental Health Hazard Assessment (OEHHA) noncancer REL for long-term exposure is 0.7 μg m^{-3} for acrolein and 5.0 μg m^{-3} for acrylonitrile, respectively (OEHHA 2019). The Texas long-term noncancer REL for methacrolein is 2.4 μg m^{-3} (TCEQ 2014). Concentrations observed in this study were consistent with those reported in Sleiman et al. (2014).

The chamber background in the THS+O$_3$ tests showed lower total carbonyl concentrations (28 μg m^{-3}), suggesting negligible long-term contamination from the previous THS aging experiment. The most prevalent carbonyls present in the blank were compounds commonly found in buildings: formaldehyde (7.8-11 ppb) and acetone (8.7-14 ppb). Furnishings did not contribute to the indoor carbonyl level. However, ozonation prior to smoking led to the formation of additional 52 μg m^{-3} of carbonyls, comparable to those formed from the subsequent THS ozonation, 53 μg m^{-3}. This is consistent with the findings by Shaughnessy et al. (2001) that formaldehyde and acetaldehyde were formed with the presence of moderate level of ozone (<115 ppb), while the level of benzaldehyde was relatively stable. The overall increase of total carbonyl concentrations also indicated that other unsaturated organic constituents in the cigarette smoke served as precursors for their formation. As a result, the irritancy/toxicity of the ozonated THS probably increased due to the more oxidized byproducts. The *AER* in this study is representative of typical indoor settings, thus providing a realistic scenario commonly found indoors.

In the THS aging experiment, the total PM mass concentrations derived from the open-faced 47-mm filters were very close to concentrations of PM$_{2.5}$ that were deduced from the IOGAPS 90-mm filters in *SHS* and *SHS/THS* samples, showing that particles larger than 2.5 μm in diameter made no significant

contributions to total PM levels in conditions where tobacco smoke was the predominant source of particles. As tobacco aerosols decreased in concentration, $PM_{2.5}$ concentrations became a smaller fraction of total PM. $PM_{2.5}$ was 85% of total PM in the *THS* sample, and 58% of total PM in the *aged THS >24h* sample. In chamber blank samples collected prior to smoking, $PM_{2.5}$ was only 28% of total PM. Total PM mass concentration increased from a low background level of 5 μg m^{-3} to 1,500 μg m^{-3} in fresh SHS, and decreased at a faster rate than ventilation removal, likely due to deposition on the chamber's surfaces, as shown in Figure 1-C. By the end of the second day, PM in aged THS decreased to a level similar to that in the chamber prior to smoking. For the THS+O$_3$ experiment conducted one month later, the chamber background remained relatively clean (9 μg m^{-3}), PM levels were not affected by the furnishings, and increased slightly by the addition of ozone before smoking (from 6.8 to 7.4 μg m^{-3}). The lower *AER* used in the THS+O$_3$ experiment allowed for a clearer observation of the effect of particle deposition after smoking took place, with a large departure of measured PM mass concentrations from the predicted values based only on ventilation removal (blue dotted line). After ozonation, PM mass concentration showed a small increase (from 8.5 to 9.5 μg m^{-3}). Hence, the formation of ultrafine particles (described below) from ozonation of adsorbed THS constituents did not result in a major change in $PM_{2.5}$ mass concentration.

3.2 Speciation of nitrogenated VOCs

Figure S3 (Supporting Information) shows the concentration of eight nitrogenated VOCs detected in the THS aging and THS+O$_3$ experiments. Note that sampling and analytical methods used in this study are different from those in Sleiman et al. (2014), in which multi-bed sorbent cartridges of Carbotrap B/Carboxen 1000 (instead of the Carbopack B/X used here) were analyzed by two-dimensional gas chromatography/time-of-flight mass spectrometry (GC $\times$ GC-TOFMS). Due to the higher sensitivity of our current measurement techniques, concentrations of eight nitrogenated VOCs in the cigarette smoke samples collected at 0.1 h, 1.2 h, 4.1 h and 29 h after smoking could be measured, in the range 0.01-100 μg m^{-3}. Compared with the initial 20 min concentrations reported in Sleiman et al. (2014), similar concentrations of nitrogenated VOCs were reported in the SHS sample, validating the repeatability of our experiment under the same conditions, i.e. the same number of cigarettes smoked in the same chamber. These eight compounds included acrylonitrile, pyridine, 3-ethylpyridine, 3-ethenylpyridine (3-EP), pyrrole, n-methylformamide, nicotine, and β-nicotyrine, all detected in the SHS and SHS/THS samples. None of these eight VOCs were detected in the chamber blank sample. 3-EP and nicotine, both cigarette smoke tracers, were observed in all post-smoking samples, with the 3EP/nicotine ratio decreasing over time. In the aged THS, all but acrylonitrile and N-methylformamide were still above the detection limit (5 ng m^{-3}), with a concentration of 3-EP ~0.1 μg m^{-3}. In the chamber background sample measured before

the THS+O_3 experiment, which was taken one month after the THS-aging experiment, seven of these nitrogenated VOCs were present, even though 3-EP, pyrrole, and β-nicotyrine had low concentrations (<0.03 μg m^{-3}). Only 3-ethylpyridine was not detected. The added furnishings didn't significantly affect the VOC concentrations for the detected nitrogenated compounds in the chamber. THS in the furnished chamber contained slightly lower levels of nitrogenated VOCs in THS compared with the unfurnished chamber, suggesting additional sorptive losses. Addition of ozone had similar effects in the furnished chamber before smoking and THS-filled chamber, diminishing the nitrogenated VOC concentrations by 4-88%.

3.3 Semivolatile compounds in denuder and filter extracts

In the THS aging experiment, GC/PCI-QQQ-MS was used to identify and quantify nitrogenated SVOCs, presented in Figure 2. Compounds detected in denuder extracts included: nicotine, cotinine (COT), hydroxycotinine (OH-COT), three tobacco-specific nitrosamines (TSNAs) including N-nitrosonornicotine (NNN), 4-(methylnitrosamino-1-(3-pyridyl)-1-butanone (NNK) and 4-(methylnitrosamino)-4-(3-pyridyl) butanal (NNA), and two TSNA degradation byproducts, 4-(methylnitrosamino)-1-(3-pyridyl)-1-butanol (NNAL), and 4-(methylnitrosamino)-4-(3-pyridyl)-1-butanol (iso-NNAL). Nicotine, COT, OH-COT and NNN were detected in the chamber blank sample before smoking, in very low levels (0.01-1 ng m^{-3}). All nitrogenated SVOC concentrations in SHS increased by one to three orders of magnitude compared with those in the chamber background, with nicotine, COT and OH-COT being the most abundant. Among the TSNAs, NNK was the most abundant species, with levels comparable with COT and OH-COT, reaching 247 ng m^{-3} in total, comprising both particle and gas phase. The high amounts of nicotine present in these samples could not be quantified accurately by this method, because the low injection temperature required to avoid thermal degradation of the TSNAs caused nicotine carryover in the inlet system. For that reason, we rely on the nicotine concentrations determined by TD-GC/MS, presented in Table S2 (Supporting Information). Those levels correspond to total airborne nicotine, which is essentially all in the gas phase, as this analyte was found primarily in denuder samples. By contrast, all other nitrogenated SVOCs were present by >93% in filter extracts of SHS. As the smoke aged, their relative fraction in the gas phase gradually increased, e.g. for NNK from 1.0% in SHS to 83% in THS, and to 100% in the aged THS (>24h) sample. These findings suggest that TSNAs and other semivolatile species adsorbed onto various indoor surfaces, and slowly partitioned back into the gas phase, consistent with the behavior observed for VOCs and carbonyls. NNA, a THS-specific TSNA (Sleiman et al. 2010b), was not detected in the gas phase of SHS and SHS/THS, probably due to its high instability at high temperatures, but it was detected in THS. The nitrosamines NNN, NNA and NNK were found to linger in THS 4-18 h after cigarette smoking, and were present in both denuder and filter extracts. NNK and NNN are known carcinogens

(Hecht 2008), and NNA has been reported to cause DNA damage (Hang 2010, Hang et al. 2013). Particle phase NNAL, a marker for NNK, was below detection limit in the THS and aged THS samples, while iso-NNAL, a potential marker for NNA, was only detected in filter extracts.

Filter extracts from the THS aging experiment were also analyzed by GC/IT-MS to identify and quantify PAHs. Figure 3 presents compounds detected in the extracts, including: naphthalene (NAP), 1-methylnaphthalene (1-MN), 2-methylnaphthalene (2-MN), acenaphthylene (ANY), acenaphthene (ANE), fluorene (FLN), phenanthrene (PHEN), fluoranthene (FLNT), pyrene (PYR), benzo[a]anthracene (B[a]A), chrysene (CHR), benzo[b]fluoranthene (B[b]F), benzo[a]pyrene (B[a]P), indeno[1,2,3-cd]pyrene (I[cd]P), and benzo[ghi]perylene (B[ghi]P). Several of these compounds were found in chamber blanks, as PAHs are commonly found in urban particulate matter. PAH concentrations increased in SHS samples over background levels, in most cases by several orders of magnitude. The denuder samples contained only the lighter fraction (2- and 3-ring PAHs), with NAP, 2-MN and 1-MN being the most abundant species. Heavier 4- and 5-ring PAHs were found only on particle extracts. From those, the 5-ring compounds were only detected in the more concentrated SHS and SHS/THS samples. Unlike TSNAs, there was little evidence of heavy PAHs partitioning to the gas phase in THS.

A) Denuder extracts
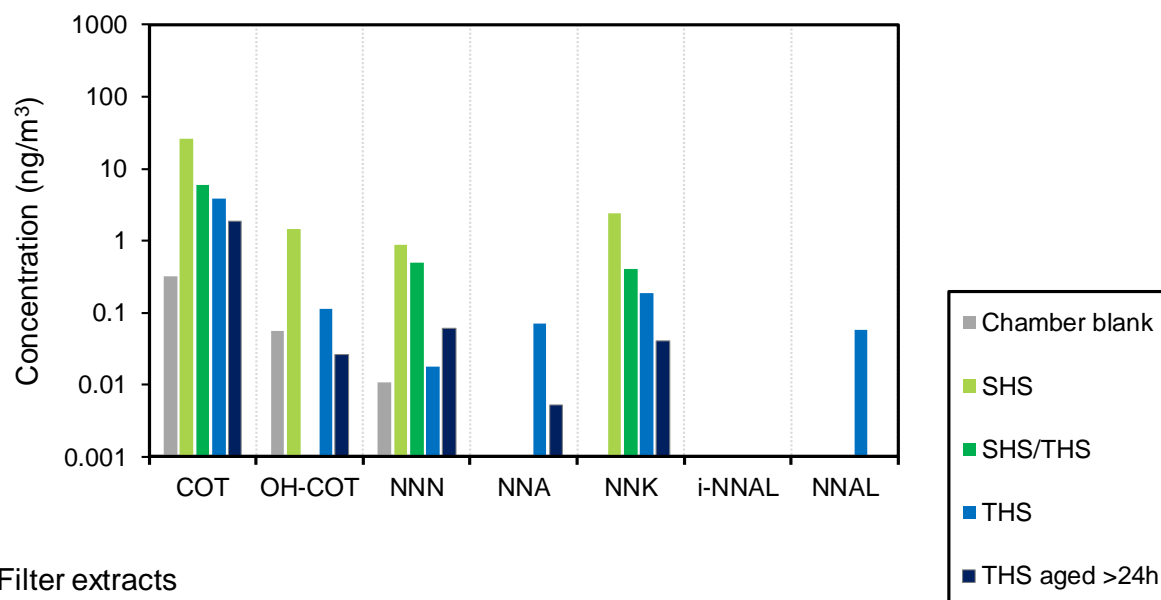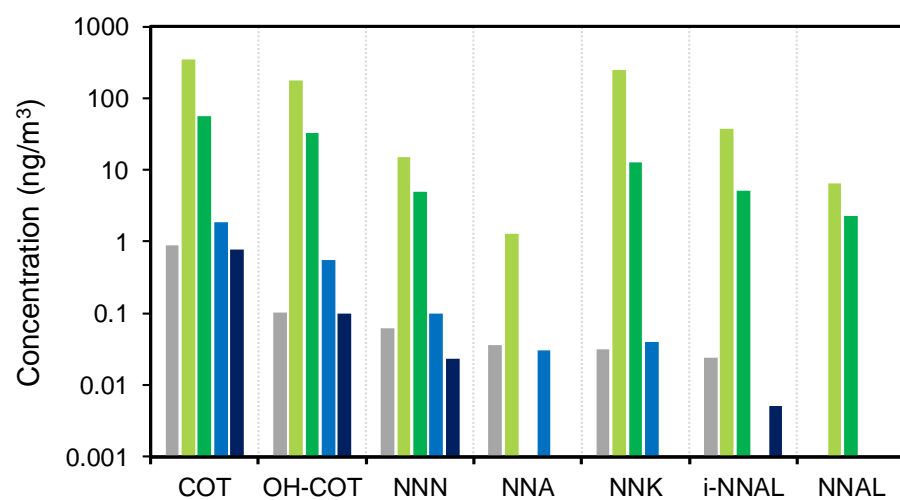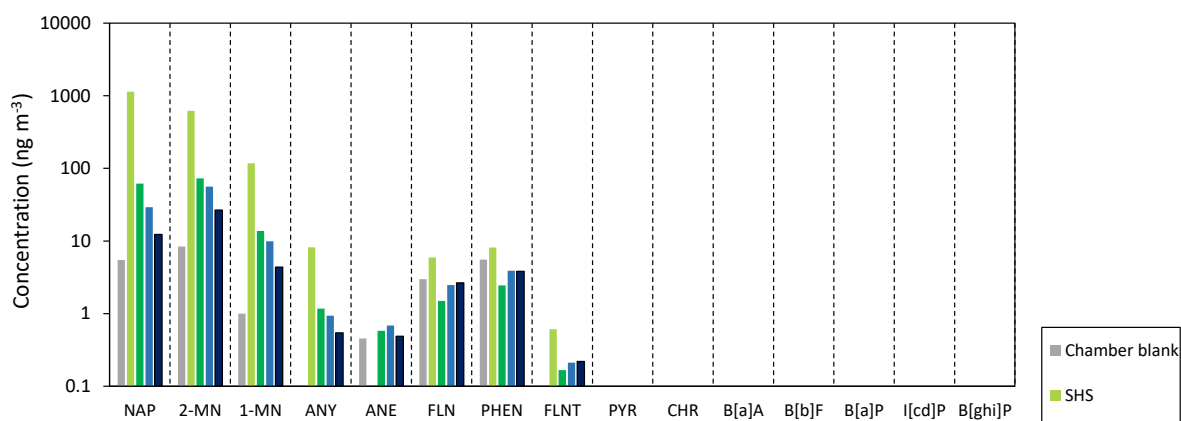

B) Filter extracts

Figure 2: Cotinine (COT), hydroxy-cotinine (OH-COT), tobacco-specific nitrosamines (TSNAs) and their degradation byproducts detected in the (A) denuder extracts and (B) filter extracts of THS aging aerosols.

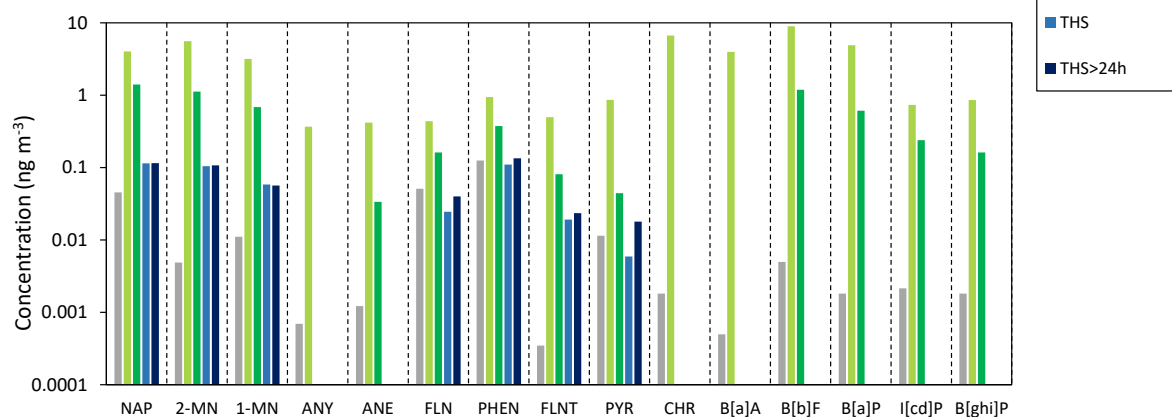A) Denuder extracts

B) Filter extracts

Figure 3: Polycyclic aromatic hydrocarbons (PAHs) detected in the (A) denuder extracts and (B) filter extracts of THS aging aerosols.

3.4 Nicotine and PAH on fabrics in THS+O₃ experiment

Species adsorbed on fabrics during the THS+O_3 experiment were analyzed by GC/IT-MS in total ion count mode, to illustrate the effects of ozonation on adsorbed species. This section describes only chemicals adsorbed onto polyester, because extracts of cotton and wool swatches could not be analyzed due to chemical interferences. Analyte concentrations were measured in µg g^{-1}, and converted to µg m^{-2} by determining the fabric weight per unit area (65 g m^{-2}). Nicotine was one of the few compounds detected on surfaces after smoking, which was not previously present on the fabric. Approximately 1 mg m^{-2} of nicotine was quantified on fabrics extracted after smoking. After ozonation, nicotine could not be detected in polyester specimens. This result is consistent with our previous observation of surface-bound nicotine reactivity with ozone (Petrick et al. 2011). Tobacco-related PAHs were also found in polyester

surfaces after smoking, but it was not possible to quantify them due to the high background. For that reason, the samples were re-analyzed in selected ion mode, following a PAH-specific procedure.

The concentration of surface-bound PAHs determined on polyester swatches by selected ion mode is reported in Figure 4. Several PAHs were found on the fabric extracts, including NAP, 2-MP, 1-MP, FLN, PHEN, ANTH, FLNT, PYR, CHR and B[a]A. All but CHR were detected in the chamber background sample, with concentrations between 0.05 and 1.1 μg per gram of fabric. All 12 PAHs have also been found in THS aging samples (Figure 3), and have previously been detected in THS-laden cotton terry cloth, at much higher mass loadings (130 ng per gram of cloth in total) (Hang et al. 2018) as a result of longer exposure duration (234 h over 1019 days) and higher exposure level. In another study, 15 PAHs, including FLN, ANTH, PHEN, FLNT, PYR, B[a]A and CHR, have also been detected in the gas- and particle-phase THS generated in the laboratory (Schick et al. 2014). In our study, after the fabrics were exposed to tobacco smoke, surface PAH concentrations increased by one order of magnitude to 0.6–22 μg per gram of fabric. Subsequent addition of ozone reduced the PAH levels on the fabrics by roughly one order of magnitude, achieving surface levels that were similar to, or lower than those prior to cigarette smoke exposure. Hence, ozonation had a positive effect in terms of removing harmful THS species from exposed surfaces.
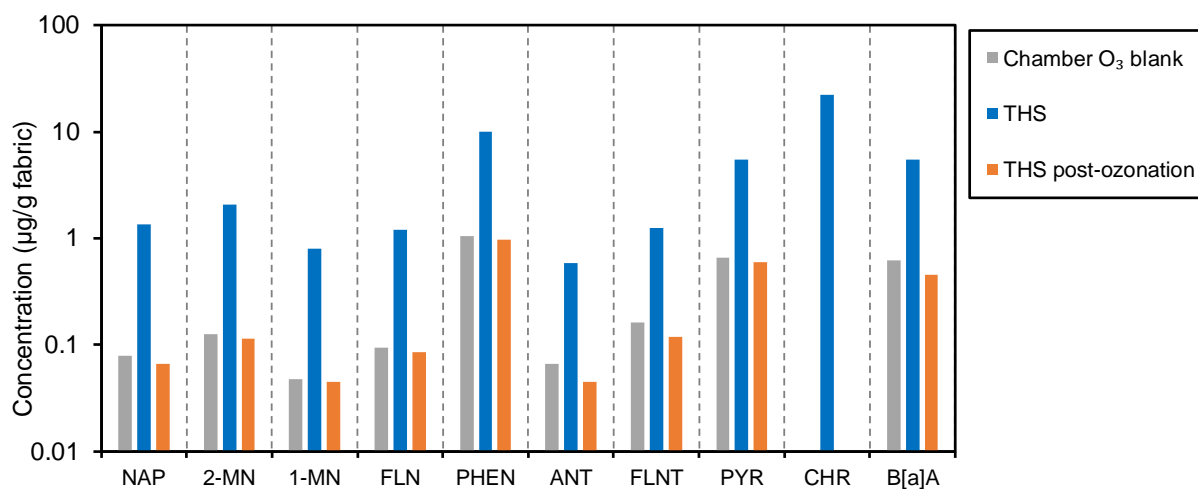

Figure 4: PAHs quantified on polyester fabrics exposed in the chamber during the THS+O₃ experiment.

3.5 Ozone and particle number concentration in the THS+O₃ experiment

Ozone was introduced in the chamber before and after smoking. Figure S4 (Supporting Information) illustrates the different concentration profiles obtained in each case. Indoor O_3 concentration reached ~180 ppb in the furnished chamber before smoking, then decayed to background concentration (~20 ppb) in about 2.5 hours. In the presence of THS, ozone concentration increased during the 60-minute operation of the ozone generator, from ~20 ppb to 135 ppb by the end of the ozone generation period. The difference between these curves (shaded area in Figure S4), allows for an estimation of the mass of ozone reacting with THS. Assuming that the amount of ozone released in both cases was the same, and that the only change in surface reactivity was due to THS, the mass of ozone consumed by reaction with THS constituents was 175 mg. This corresponds to approximately 58% of the total ozone released by the device (300 mg h^{-1}).

The decay of ozone was fast, reaching the background plateau (~30 ppb) in about an hour. The total particle number concentration started increasing rapidly when indoor O_3 reached ~85 ppb, and its peak appeared ~0.3 hour after ozonation ended. The time required for the particles to return to background levels was also longer than for O_3, approximately 2 hours (Figure 5-A). The size-resolved particle number distribution is shown in Figure 5-B. Before and during the ozone introduction, particle size range was between 20 and 200 nm in diameter, mostly below 120 nm. The secondary organic aerosol formed as a result of ozone addition was almost all in the ultrafine range (<100 nm), with the mode diameter between 20 and 60 nm, similar to the 60 nm diameter observed in the SHS ozonolysis experiment conducted previously by our group (Sleiman et al. 2010a). No aging effects were observed in the particle size distribution during the four hours after ozone was introduced.
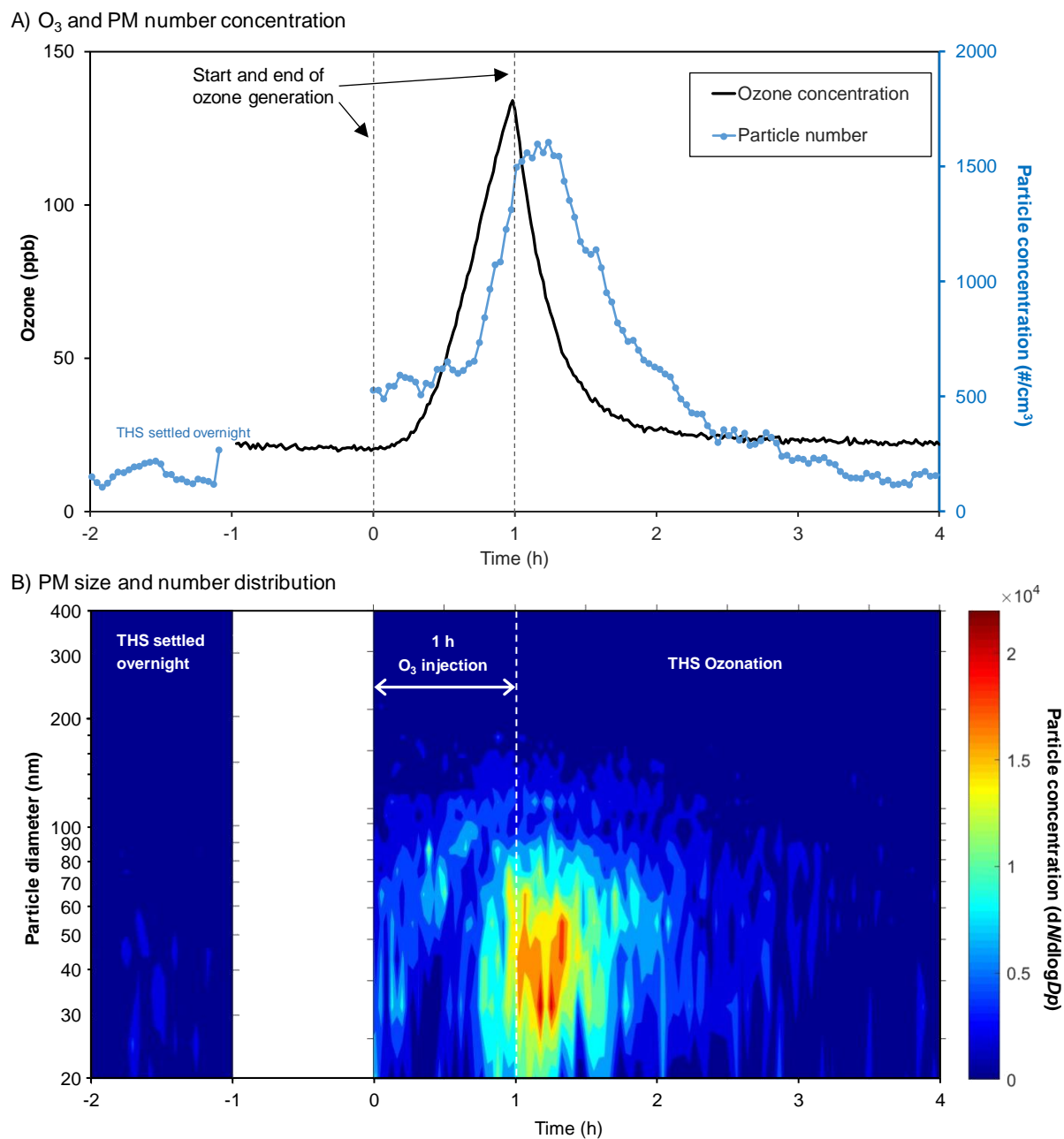
A) O$_3$ and PM number concentration

B) PM size and number distribution

Figure 5: (A) Ozone concentration (black) and total particle number concentration (blue) in the THS+O$_3$ experiment. (B) Evolution of particle size and number distribution of THS in the chamber before and after the injection of O$_3$.

The evolution of indoor pollutant concentrations after ozonation can be described by a pseudo first-order removal process, assuming uniform mixing in the indoor environment. The loss is due to the combined effects of interaction with indoor surfaces and air exchange. Ozone deposition velocity to surfaces, v_d (expressed in m h^{-1}), can be determined with the measured ozone concentrations, chamber surface area, chamber volume, and air exchange rate, by applying a time-dependent material balance for ozone in chamber air, shown in Equations 1 and 2:

$$\frac{dC_t}{dt} = AER\left(C_{supply} - C_t\right) - kC_t \tag{1}$$

$$v_d = k/(\frac{S}{V}) \tag{2}$$

where C_t is the ozone concentration in the chamber (ppb), C_{supply} is the supply ozone concentration in ventilation air, assumed to be 0 ppb in this case, S is surface area (m^2) inside the chamber, including the furnishings, k is O$_3$ decay rate (h^{-1}), V is chamber volume (m^3), and AER is air exchange rate (h^{-1}). By applying an exponential fit to the decay curve of O$_3$ shown in Figure 5-A, the O$_3$ decay rate, k, was determined to be 2.98 h^{-1}, after accounting for the air change rate, which was determined separately (0.17 h^{-1}). Then, the O$_3$ deposition velocity, v_d (m h^{-1}), was calculated using Equation (2) as 0.84 m h^{-1} (0.023 cm s^{-1}). The measured O$_3$ decay rate was well within the range of 1.4 h^{-1} to 7.6 h^{-1} as summarized in Weschler (2000). Nazaroff et al. (1993) reported O$_3$ deposition velocities using estimated surface-area-to-volume (S/V) ratios from several studies, ranging from 0.015 cm s^{-1} in a stainless steel room to 0.075 cm s^{-1} in a highly ventilated cleanroom. Considering that the wall material of the chamber was drywall painted many years ago, with estimated ozone deposition velocity of 0.03-0.042 cm s^{-1} or lower for aged material (Grøntoft and Raychaudhuri 2004), our measured overall ozone deposition velocity is a reasonable value.

Similarly, the particle deposition rate was calculated as 1.29 h^{-1}, and particle deposition velocity was 0.30 m h^{-1} (0.008 cm s^{-1}). Fine particle deposition velocity was measured previously in commercial buildings, apartment, and museums, as summarized in Nazaroff et al. (1993), ranging from 0.0002 to 0.005 cm s^{-1}. Deposition rate of ultrafine particles was measured in an environmental chamber, between 0.2 and 1 h^{-1} (Fig. 7 in Mosley et al. 2001), i.e. 0.001 – 0.006 cm s^{-1}, with only linoleum floor and gypsum board walls as the available deposition surfaces. As the roughness of the added furnishings was higher than the chamber interior surfaces, our measured deposition velocity is realistic.

Considering that ozone generators are used in the decontamination and restoration processes, it is necessary to determine a minimum safe re-entry time for occupants or professionals who handle the ozonation procedure to return indoors. Here, we define the minimum re-entry time as the time needed for O$_3$ (t_{O_3}) and particulate matter (t_{PM}) to decrease to 10% of their peak concentration (C_{max}, Equation 3),

$$C_t = C_{max} \times 0.1 \tag{3}$$

Applying the calculated O_3 and particle deposition velocities to indoor environments with varying *S/V* ratio and *AER*, we calculated t_{O_3} and t_{PM} using Eq. (1). Previous researchers have reported *S/V* ratios ranging from 1.2 to 4.6 m^{-1} for residential indoor environments (Lee et al. 1999, Singer et al. 2007), so the range of *S/V* ratio was chosen between 1.5-3.0 m^{-1}, and *AER* between 0.1-3.0 h^{-1}. Mean residential *AER* values are typically between 0.5 and 1.7 h^{-1}, and mean nonresidential values between 1.5 and 2.0 h^{-1} (Weschler 2006). Lower *AER* (e.g. 0.2 h^{-1}) is now common in energy-efficient residential construction.

The calculated t_{O_3} and t_P are shown in 2-D contour plots in Figures 6-A and 6-B. It can be seen that it takes longer for PM than for ozone to decay to a safer re-entry level. For example, in a small room with *S/V* = 1.5 and an *AER* of 0.5, the estimated minimum re-entry time is 2.1 h for PM, which is ~65% longer than that of ozone (1.3 h). The relative difference R_t between t_{O_3} and t_{PM} was calculated with Equation (4), showing that t_{PM} was 70% to 150% longer than t_{O_3}. A lag time of 0.3 h has been added to t_{PM}, the minimum re-entry time calculated with PM, considering that the peak PM concentration was not reached until 0.3 h after the O_3 concentration peaked at the end of the ozonation period.

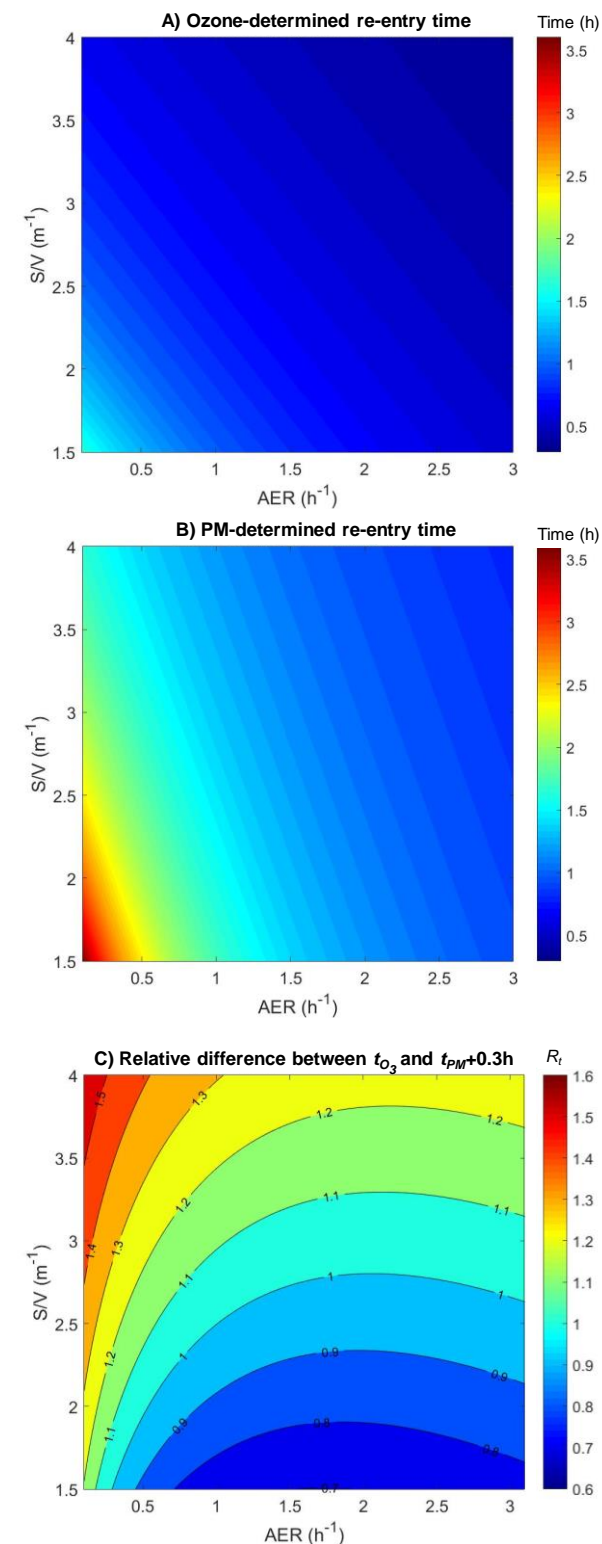$$R_t = \left(t_{PM} + 0.3 - t_{O_3}\right)/t_{O_3} \tag{4}$$

Figure 6: Calculated minimum re-entry time (h) based on (A) the indoor ozone concentration, and (B) PM concentrations. The relative difference between t_{O_3} and $t_{PM}+0.3h$ is plotted in panel (C). A minimum safe re-entry time is arbitrarily determined as the time needed for O_3 or PM concentrations to be reduced to 10% of the peak concentration.

4. Conclusions

THS aerosols change chemically as they age, being enriched in less volatile species. VOCs and volatile carbonyls initially decayed faster in the chamber, compared with concentrations estimated by ventilation alone. However, aged THS samples showed higher levels of VOC than their predicted air-exchange-diluted concentration. These observations indicate dynamic partitioning of these compounds between the gas phase and the surfaces, leading to inhalation exposures that largely exceed the duration of smoking events. This is consistent with the well documented role of indoor surfaces as reservoirs of THS contamination (Jacob et al. 2017).

Addition of ozone into the THS-contaminated environment led to formation of secondary organic aerosol, and increased concentration of TVOC, carbonyls and PM (mostly ultrafine particles). This likely increases the irritating and toxic nature of THS, suggesting that there may be risks associated with re-entering the space even after residual ozone was consumed. Thus, benefits of THS remediation using ozonation should be weighed with these potential health risks.

Smoking-generated nicotine and PAHs that adsorbed onto polyester fabrics were effectively eliminated from the surfaces by the ozonation process, reducing their concentration to background levels. This result suggests that ozonation may not only be effective in removing unpleasant odors, but can also mitigate exposures to harmful chemicals adsorbed on indoor surfaces. However, further investigation of potential ozonation byproducts formed in these reactions is needed.

5. Acknowledgements

6. References

Bahl, V., P. Jacob, 3rd, C. Havel, S. F. Schick and P. Talbot, 2014. Thirdhand cigarette smoke: factors affecting exposure and remediation. PloS ONE 9(10): e108258-e108258. DOI: 10.1371/journal.pone.0108258.

Borduas, N., J. G. Murphy, C. Wang, G. da Silva and J. P. D. Abbatt, 2016. Gas Phase Oxidation of Nicotine by OH Radicals: Kinetics, Mechanisms, and Formation of HNCO. Environmental Science & Technology Letters 3(9): 327-331.

Britigan, N., A. Alshawa and S. A. Nizkorodov, 2006. Quantification of ozone levels in indoor environments generated by ionization and ozonolysis air purifiers. Journal of the Air & Waste Management Association 56(5): 601-610. DOI: 10.1080/10473289.2006.10464467.

Brodowska, A. J., A. Nowak and K. Śmigielski, 2018. Ozone in the food industry: Principles of ozone treatment, mechanisms of action, and applications: An overview. Critical Reviews in Food Science and Nutrition 58(13): 2176-2201. DOI: 10.1080/10408398.2017.1308313.

CARB. (2020). Hazardous Ozone-Generating "Air Purifiers". URL: https://ww2.arb.ca.gov/our-work/programs/air-cleaners-ozone-products/hazardous-ozone-generating-air-purifiers. (Accessed on October 10, 2020)

Coleman, B. K., M. M. Lunden, H. Destaillats and W. W. Nazaroff, 2008. Secondary organic aerosol from ozone-initiated reactions with terpene-rich household products. Atmospheric Environment 42(35): 8234-8245.

Collins, D. B., C. Wang and J. P. D. Abbatt, 2018. Selective uptake of third-hand tobacco smoke components to inorganic and organic aerosol particles. Environ. Sci. Technol. 52: 13195-13201. DOI: 10.1021/acs.est.8b03880.

DeCarlo, P., A. M. Avery and M. S. Waring, 2018. Thirdhand smoke uptake to aerosol particles in the indoor environment. Sci. Adv. 4(5): eaap8368. DOI: 10.1126/sciadv.aap8368.

Destaillats, H., R. L. Maddalena, B. C. Singer, A. T. Hodgson and T. E. McKone, 2008. Indoor pollutants emitted by office equipment: A review of reported data and information needs. Atmospheric Environment 42(7): 1371-1388. DOI: 10.1016/j.atmosenv.2007.10.080.

Destaillats, H., B. C. Singer, S. K. Lee and L. A. Gundel, 2006. Effect of ozone on nicotine desorption from model surfaces: Evidence for heterogeneous chemistry. Environmental Science & Technology 40(6): 1799-1805.

EPA (1984). Method TO-1, Revision 1,0: Method for the Determination of Volatile Organic Compounds in Ambient Air Using Tenax® Adsorption and Gas Chromatography/Mass Spectrometry (GC/ MS). Cincinnati, OH, Center for Environmental Research Information, Office of Research and Development, U.S. Environmental Protection Agency (U.S. EPA).

EPA (1999). Compendium Method TO-11A - Determination of Formaldehyde in Ambient Air Using Adsorbent Cartridge Followed by HPLC [Active Sampling Methodology]. Cincinnati, OH, Office of Research and Development, U.S. Environmental Protection Agency (U.S. EPA).

Fan, Z. H., P. Lioy, C. Weschler, N. Fiedler, H. Kipen and J. F. Zhang, 2003. Ozone-initiated reactions with mixtures of volatile organic compounds under simulated indoor conditions. Environmental Science & Technology 37(9): 1811-1821. DOI: 10.1021/es026231i.

Grøntoft, T. and M. R. Raychaudhuri, 2004. Compilation of tables of surface deposition velocities for O_3, NO_2 and SO_2 to a range of indoor surfaces. Atmospheric Environment 38(4): 533-544. DOI: 10.1016/j.atmosenv.2003.10.010.

Gundel, L. A., V. C. Lee, K. R. R. Mahanama, R. K. Stevens and J. M. Daisey, 1995. Direct determination of the phase distributions of semi-volatile polycyclic aromatic hydrocarbons using annular denuders. Atmospheric Environment 29(14): 1719-1733. DOI: 10.1016/1352-2310(94)00366-S.

Guo, C., Z. Gao and J. Shen, 2019. Emission rates of indoor ozone emission devices: A literature review. Building and Environment 158: 302-318. DOI: 10.1016/j.buildenv.2019.05.024.

Hang, B., 2010. Formation and repair of tobacco carcinogen-derived bulky DNA adducts. J Nucleic Acids 2010: 709521. DOI: 10.4061/2010/709521.

Hang, B., A. H. Sarker, C. Havel, S. Saha, T. K. Hazra, S. Schick, P. Jacob, V. Rehan, A. Chenna, D. Sharan, M. Sleiman, H. Destaillats and L. A. Gundel, 2013. Thirdhand smoke causes DNA damage in human cells. Mutagenesis 28(4). DOI: 10.1093/mutage/get013.

Hang, B., Y. Wang, Y. Huang, P. Wang, S. A. Langley, L. Bi, A. H. Sarker, S. F. Schick, C. Havel, P. Jacob, 3rd, N. Benowitz, H. Destaillats, X. Tang, Y. Xia, K. Y. Jen, L. A. Gundel, J. H. Mao and A. M.

Snijders, 2018. Short-term early exposure to thirdhand cigarette smoke increases lung cancer incidence in mice. Clin Sci (Lond) 132(4): 475-488. DOI: 10.1042/CS20171521.

Hecht, S. S., 2008. Progress and challenges in selected areas of tobacco carcinogenesis. Chem Res Toxicol 21(1): 160-171. DOI: 10.1021/tx7002068.

Hoh, E., R. N. Hunt, P. J. E. Quintana, J. M. Zakarian, D. A. Chatfield, B. C. Wittry, E. Rodriguez and G. E. Matt, 2012. Environmental Tobacco Smoke as a Source of Polycyclic Aromatic Hydrocarbons in Settled Household Dust. Environmental Science & Technology 46(7): 4174-4183. DOI: 10.1021/es300267g.

Hubbard, H. F., B. K. Coleman, G. Sarwar and R. L. Corsi, 2005. Effects of an ozone-generating air purifier on indoor secondary particles in three residential dwellings. Indoor Air 15(6): 432-444.

Jacob, P., N. Benowitz, H. Destaillats, L. A. Gundel, B. Hang, M. Martins-Green, G. E. Matt, P. J. E. Quintana, J. Samet, S. Schick, P. Talbot, N. J. Aquilina, M. F. Hovell, J.-H. Mao and T. P. Whitehead, 2017. Thirdhand smoke: New evidence, challenges and future directions. Chem. Res. Toxicol. 30: 270-294. DOI: 10.1021/acs.chemrestox.6b00343.

Koop, C. E., 1986. The health consequences of involuntary smoking : a report of the Surgeon General, 1986.

Lee, K., J. Vallarino, T. Dumyahn, H. Ozkaynak and J. D. Spengler, 1999. Ozone decay rates in residences. J Air Waste Manag Assoc 49(10): 1238-1244. DOI: 10.1080/10473289.1999.10463913.

Matt, G. E., P. J. E. Quintana, H. Destaillats, L. A. Gundel, M. Sleiman, B. C. Singer, P. Jacob, N. Benowitz, J. P. Winikoff, V. Rehan, P. Talbot, S. Schick, J. Samet, Y. Wang, B. Hang, M. Martins-Green, J. F. Pankow and M. F. Hovell, 2011. Thirdhand tobacco smoke: Emerging evidence and arguments for a multidisciplinary research agenda. Environmental Health Perspectives 119: 1218-1226.

Matt, G. E., P. J. E. Quintana, E. Hoh, J. M. Zakarian, Z. Chowdhury, M. F. Hovell, P. Jacob, K. Watanabe, T. S. Theweny, V. Flores, A. Nguyen, N. Dhaliwal and G. Hayward, 2018. A Casino goes smoke free: a longitudinal study of secondhand and thirdhand smoke pollution and exposure. Tobacco Control 27(6): 643. DOI: 10.1136/tobaccocontrol-2017-054052.

Matt, G. E., P. J. E. Quintana, J. M. Zakarian, E. Hoh, M. F. Hovell, M. Mahabee-Gittens, K. Watanabe, K. Datuin, C. Vue and D. A. Chatfield, 2017. When smokers quit: exposure to nicotine and carcinogens

persists from thirdhand smoke pollution. Tobacco Control 26(5): 548. DOI: 10.1136/tobaccocontrol-2016-053119.

Morrison, G. C. and W. W. Nazaroff, 2002. Ozone interactions with carpet: secondary emissions of aldehydes. Environ Sci Technol 36(10): 2185-2192. DOI: 10.1021/es0113089.

Mosley, R. B., D. J. Greenwell, L. E. Sparks, Z. Guo, W. G. Tucker, R. Fortmann and C. Whitfield, 2001. Penetration of Ambient Fine Particles into the Indoor Environment. Aerosol Science and Technology 34(1): 127-136. DOI: 10.1080/02786820117449.

Nazaroff, W. W., A. J. Gadgil and C. J. Weschler (1993). Critique of the use of deposition velocity in modeling indoor air quality. United States, American Society for Testing and Materials.

Nazaroff, W. W. and C. J. Weschler, 2004. Cleaning products and air fresheners: exposure to primary and secondary air pollutants. Atmospheric Environment 38(18): 2841-2865. DOI: 10.1016/j.atmosenv.2004.02.040.

Niu, J. L., T. C. W. Tung and J. Burnett, 2001. Quantification of dust removal and ozone emission of ionizer air-cleaners by chamber testing. Journal of Electrostatics 51: 20-24.

OEHHA. (2019). OEHHA Acute, 8-hour and Chronic Reference Exposure Level (REL) Summary. URL: https://oehha.ca.gov/air/general-info/oehha-acute-8-hour-and-chronic-reference-exposure-level-rel-summary. (Accessed on October 10, 2020)

Petrick, L. M., M. Sleiman, Y. Dubowski, L. A. Gundel and H. Destaillats, 2011. Tobacco smoke aging in the presence of ozone: A room-sized chamber study. Atmospheric Environment 45(28): 4959-4965. DOI: 10.1016/j.atmosenv.2011.05.076.

Poppendieck, D. G., D. Rim and A. K. Persily, 2014. Ultrafine Particle Removal and Ozone Generation by In-Duct Electrostatic Precipitators. Environmental Science & Technology 48(3): 2067-2074. DOI: 10.1021/es404884p.

Rim, D., E. T. Gall, R. L. Maddalena and W. W. Nazaroff, 2016. Ozone reaction with interior building materials: Influence of diurnal ozone variation, temperature and humidity. Atmospheric Environment 125(Part A): 15-23. DOI: 10.1016/j.atmosenv.2015.10.093.

Sarwar, G., R. Corsi, D. Allen and C. Weschler, 2003. The significance of secondary organic aerosol formation and growth in buildings: experimental and computational evidence. Atmospheric Environment 37(9-10): 1365-1381.

Schick, S. F., K. F. Farraro, C. Perrino, M. Sleiman, G. van de Vossenberg, M. P. Trinh, S. K. Hammond, B. M. Jenkins and J. Balmes, 2014. Thirdhand cigarette smoke in an experimental chamber: evidence of surface deposition of nicotine, nitrosamines and polycyclic aromatic hydrocarbons and de novo formation of NNK. Tobacco Control 23(2): 152. DOI: 10.1136/tobaccocontrol-2012-050915.

Serra, R., L. Abrunhosa, Z. Kozakiewicz, A. Venancio and N. Lima, 2003. Use of ozone to reduce molds in a cheese ripening room. Journal of Food Protection 66(12): 2355-2358. DOI: Doi 10.4315/0362-028x-66.12.2355.

Shaughnessy, R. J., T. J. McDaniels and C. J. Weschler, 2001. Indoor Chemistry: Ozone and Volatile Organic Compounds Found in Tobacco Smoke. Environmental Science & Technology 35(13): 2758-2764. DOI: 10.1021/es001896a.

Sheu, R., C. Stönner, J. C. Ditto, T. Klüpfel, J. Williams and D. R. Gentner, 2020. Human transport of thirdhand tobacco smoke: A prominent source of hazardous air pollutants into indoor nonsmoking environments. Science Advances 6(10): eaay4109. DOI: 10.1126/sciadv.aay4109.

Singer, B. C., B. K. Coleman, H. Destaillats, A. T. Hodgson, M. M. Lunden, C. J. Weschler and W. W. Nazaroff, 2006. Indoor secondary pollutants from cleaning product and air freshener use in the presence of ozone. Atmospheric Environment 40(35): 6696-6710.

Singer, B. C., A. T. Hodgson, T. Hotchi, K. Y. Ming, R. G. Sextro, E. E. Wood and N. J. Brown, 2007. Sorption of organic gases in residential rooms. Atmospheric Environment 41(15): 3251-3265. DOI: 10.1016/j.atmosenv.2006.07.056.

Singer, B. C., K. L. Revzan, T. Hotchi, A. T. Hodgson and N. J. Brown, 2004. Sorption of organic gases in a furnished room. Atmospheric Environment 38(16): 2483-2494.

Sleiman, M., H. Destaillats, J. D. Smith, C.-L. Liu, M. Ahmed, K. R. Wilson and L. A. Gundel, 2010a. Secondary organic aerosol formation from ozone-initiated reactions with nicotine and secondhand tobacco smoke. Atmospheric Environment 44(34): 4191-4198. DOI: 10.1016/j.atmosenv.2010.07.023.

Sleiman, M., L. A. Gundel, J. F. Pankow, P. Jacob, B. C. Singer and H. Destaillats, 2010b. Formation of carcinogens indoors by surface-mediated reactions of nicotine with nitrous acid, leading to potential thirdhand smoke hazards. Proceedings of the National Academy of Sciences USA 107(15): 6576-6581. DOI: 10.1073/pnas.0912820107.

Sleiman, M., J. M. Logue, W. T. Luo, J. F. Pankow, L. A. Gundel and H. Destaillats, 2014. Inhalable Constituents of Thirdhand Tobacco Smoke: Chemical Characterization and Health Impact Considerations. Environmental Science & Technology 48(22): 13093-13101.

Stephens, B., E. T. Gall and J. A. Siegel, 2012. Measuring the Penetration of Ambient Ozone into Residential Buildings. Environmental Science & Technology 46(2): 929-936. DOI: 10.1021/es2028795.

Swartz, E., L. Stockburger and L. A. Gundel, 2003. Recovery of semivolatile organic compounds during sample preparation: Implications for characterization of airborne particulate matter. Environmental Science and Technology 37(3): 597-605. DOI: 10.1021/es011128z.

TCEQ. (2014). Texas Commission on Environmental Quality Development Support Document. URL: https://www.tceq.texas.gov/assets/public/implementation/tox/dsd/final/methacrolein.pdf. (Accessed on October 10, 2020)

Tung, T. C. W., J. L. Niu, J. Burnett and K. Hung, 2005. Determination of ozone emission from a domestic air cleaner and decay parameters using environmental chamber tests. Indoor and Built Environment 14(1): 29-37.

U.S. Department of Health and Human Services,2006. The Health Consequences of Involuntary Exposure to Tobacco Smoke: A Report of the Surgeon General. Atlanta, GA: U.S. Department of Health and Human Services, Centers for Disease Control and Prevention, Coordinating Center for Health Promotion, National Center for Chronic Disease Prevention and Health Promotion, Office on Smoking and Health. https://www.ncbi.nlm.nih.gov/books/NBK44324/. (Accessed on October 10, 2020)

Wang, H., C. R. He, L. Morawska, P. McGarry and G. Johnson, 2012. Ozone-Initiated Particle Formation, Particle Aging, and Precursors in a Laser Printer. Environmental Science & Technology 46(2): 704-712. DOI: 10.1021/es203066k.

Wang, H. and G. C. Morrison, 2006. Ozone-initiated secondary emission rates of aldehydes from indoor surfaces in four homes. Environ Sci Technol 40(17): 5263-5268. DOI: 10.1021/es060080s.

Waring, M. S. and J. A. Siegel, 2011. The effect of an ion generator on indoor air quality in a residential room. Indoor Air 21(4): 267-276. DOI: 10.1111/j.1600-0668.2010.00696.x.

Weschler, C. J., 2000. Ozone in indoor environments: concentration and chemistry. Indoor Air 10(4): 269-288. DOI: 10.1034/j.1600-0668.2000.010004269.x.

Weschler, C. J., 2006. Ozone's Impact on Public Health: Contributions from Indoor Exposures to Ozone and Products of Ozone-Initiated Chemistry. Environmental Health Perspectives 114(10): 1489-1496. DOI: doi:10.1289/ehp.9256.

Weschler, C. J. and N. Carslaw, 2018. Indoor Chemistry. Environmental Science & Technology 52(5): 2419-2428. DOI: 10.1021/acs.est.7b06387.

Wisthaler, A. and C. J. Weschler, 2010. Reactions of ozone with human skin lipids: Sources of carbonyls, dicarbonyls, and hydroxycarbonyls in indoor air. Proceedings of the National Academy of Sciences 107(15): 6568-6575. DOI: 10.1073/pnas.0904498106.

Zhang, J. and P. J. Lioy, 1994. Ozone in Residential Air: Concentrations, I/O Ratios, Indoor Chemistry, and Exposures. Indoor Air 4(2): 95-105. DOI: 10.1111/j.1600-0668.1994.t01-2-00004.x.

Zhang, Q. and P. L. Jenkins, 2017. Evaluation of ozone emissions and exposures from consumer products and home appliances. Indoor Air 27(2): 386-397.

SUPPORTING INFORMATION

Chemical changes in thirdhand smoke associated with remediation using an ozone generator

Xiaochen Tang[a,*], Noelia Ramirez Gonzalez[b,c], Marion L. Russell[a],
Randy L. Maddalena[a], Lara A. Gundel[a], Hugo Destaillats[a,*]

[a] Indoor Environment Group, Lawrence Berkeley National Laboratory,
Berkeley, California, USA
[b] Institut d'Investigació Sanitària Pere Virgili, Tarragona, Spain
[c] Universitat Rovira i Virgili, Department of Electronic Engineering,
MIL@b, CIBERDEM, Tarragona, Spain

[*]*Corresponding authors*

Email: XTang@lbl.gov, HDestaillats@lbl.gov

Mailing Address: 1 Cyclotron Rd, M/S 70R0108B, Berkeley, CA 94720

Table S1. Start time and duration of PM, VOC and carbonyl samples in each phase of the THS aging and THS+O_3 experiments. Six smoldering cigarettes were consumed by t = 0 h.

| Experiment	Samples	Start time (h)	Sampling duration (h)		
			PM	**VOC**	**Carbonyls**
THS Aging	Chamber blank	-20	18	4.1	3.9
	[smoking at t= 0 h]				
	SHS	0.1	0.4	0.3	0.4
	SHS/THS transition	1.2	2.1	1.1	2.1
	THS	4.1	14	14	14
	THS aged >24 h	19	24	24	24
THS+O_3	*[1-h ozonation for chamber quenching]*				
	Chamber blank	-27	1.9	2.4	2.4
	Chamber blank + furnishing	-10	2.4	2.4	2.4
	[1-h ozonation starting at t= -5.3 h]				
	Chamber blank+ furnishing + O_3	-4.1	2.3	2.3	2.3
	[smoking at t= 0 h]				
	THS	14	2.3	2.3	2.3
	[1-h ozonation starting at t= 17.2 h]				
	THS post-ozonation	19	2.1	2.1	2.1
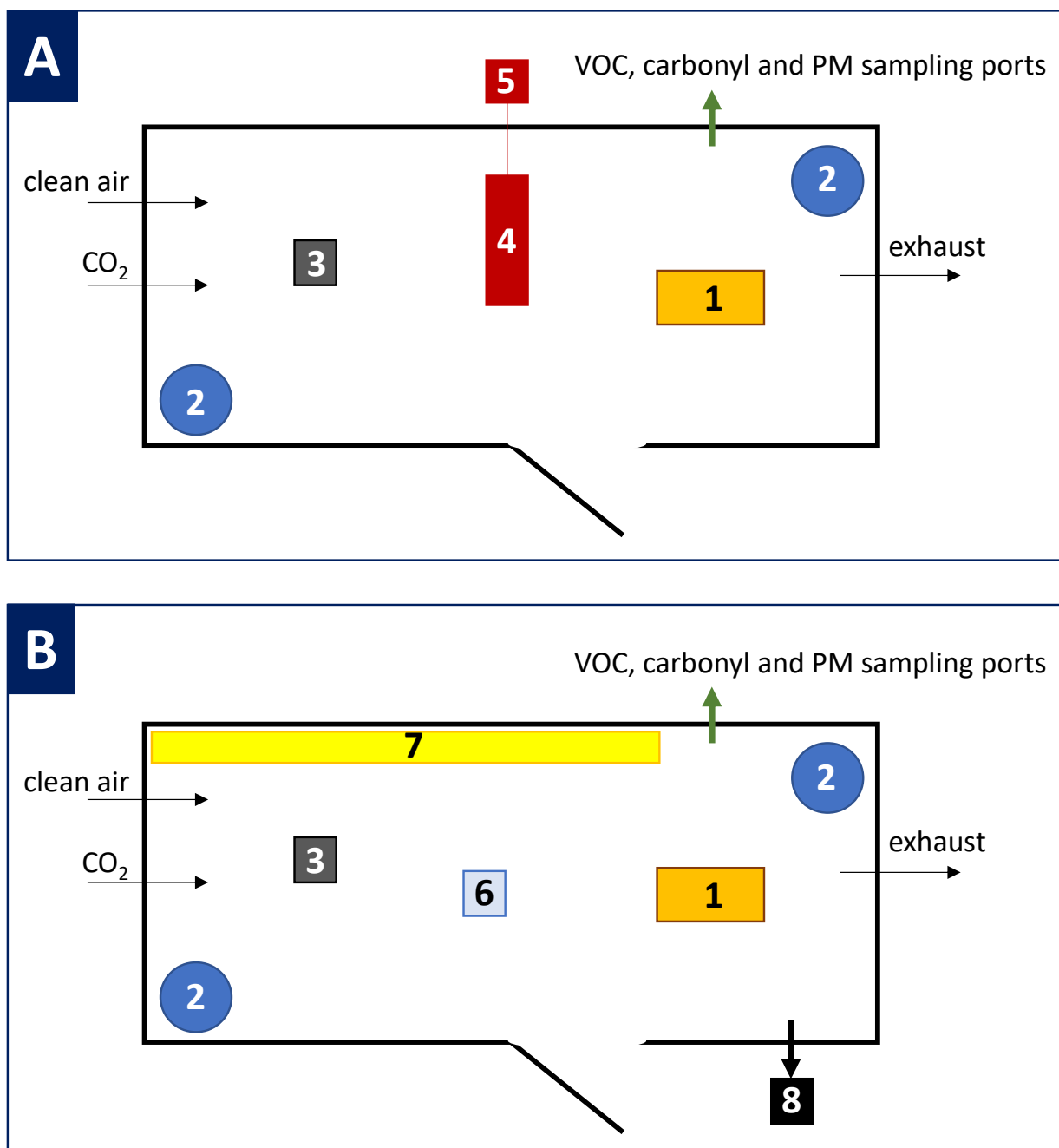
Figure S1: Configuration of room-sized experimental chamber in (A) the THS aging experiment, and (B) the THS+O_3 experiment. 1: Table where cigarettes were consumed; 2: mixing fans; 3: CO_2 sensor; 4: IOGAPS; 5: high-volume pump; 6: ozone generator; 7: fabrics; 8: aerosol instruments (SMPS/CPC).

Table S2. VOC concentration (μg m^{-3}) measured by TD-GCMS in the THS aging and THS+O$_3$ experiment.

Chemical	THS aging					THS + O$_3$				
	Chamber blank	SHS	SHS/THS	THS	THS aged >24 h	Chamber blank	Chamber blank + furnishing	Chamber blank + furnishing + O$_3$	THS	THS post-ozonation
Isoprene (ISO)	0.28	1264	799	95	1.9	0.89	1.4	2.0	100	19
Acrylonitrile (ACRY)	BDL[a]	53	34	6.8	BDL	0.99	3.7	0.78	13.1	4.7
Pyridine (PRY)	0.006	73	28	2.3	0.83	0.091	0.26	BDL	1.2	1.12
2,3-Dimethylpyridine (2,3-DMP)	BDL	1.8	0.44	0.07	BDL	BDL	BDL	0.01	BDL	BDL
3-Ethylpyridine (3-ETP)	BDL	6.4	1.9	0.31	0.094	BDL	BDL	BDL	0.14	0.10
3-Ethenylpyridine (3-EP)	BDL	66	21	4.0	1.2	0.011	0.025	BDL	2.3	1.5
Pyrrole (PYL)	BDL	40	24	5.3	0.59	0.021	0.056	BDL	4.4	0.54
N-Methylformamide (N-MF)	BDL	1.8	0.66	BDL	BDL	0.12	0.22	0.19	0.43	0.35
Nicotine (NIC)	BDL	61	21	5.9	2.7	0.14	0.22	BDL	6.2	3.5
β-Nicotyrine (β-NIC)	BDL	6.6	2.7	0.90	0.39	0.020	BDL	BDL	0.61	0.38
TVOC (toluene equivalent)[b]	16	2320	1145	278	80	68	54	150	225	354

a. BDL: below detection limit
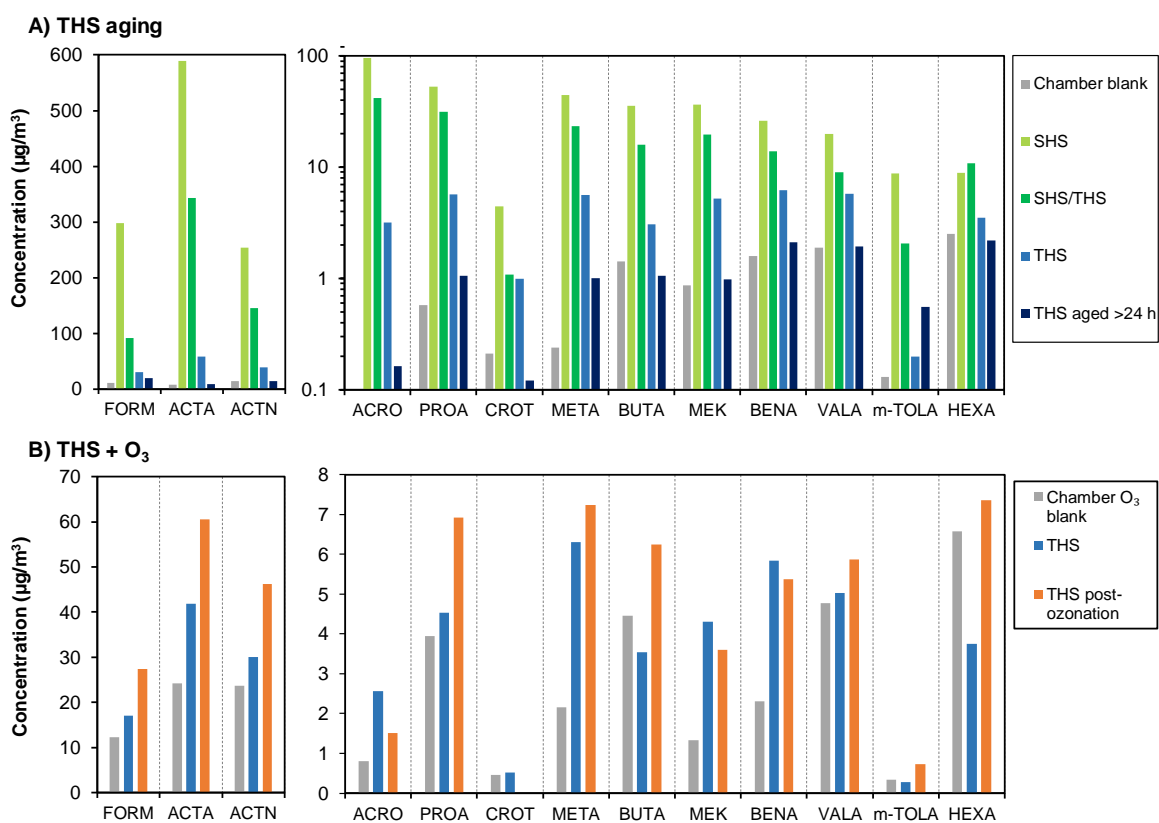b. TVOC (toluene equivalent): See Section 2.5.1 for a description

Figure S2: Volatile carbonyls concentration (μg m^{-3}) measured in (A) THS aging and (B) THS+O$_3$ experiment.

Table S3. Volatile carbonyl concentration (μg m^{-3}) measured in the THS aging and THS+O$_3$ experiments.

Chemical	THS aging					THS + O$_3$				
	Chamber blank	SHS	SHS/THS	THS	THS aged >24 h	Chamber blank	Chamber blank + furnishing	Chamber blank + furnishing + O$_3$	THS	THS post-ozonation
Formaldehyde (FORM)	11	298	92	30	19	7.9	8.1	12	17	27
Acetaldehyde (ACTA)	8.3	589	343	58	9.3	4.6	4.6	24	42	60
Acetone (ACTN)	14	254	146	39	15	8.7	11	24	30	46
Acrolein (ACRO)	BDL[a]	96	41.8	3.2	0.16	0.20	0.40	0.81	2.6	1.5
Propionaldehyde (PROA)	0.57	53	31	5.7	1.1	0.61	0.79	3.9	4.5	6.9
Crotonaldehyde (CROT)	0.21	4.5	1.1	1.0	0.12	BDL	0.20	0.46	0.53	BDL
Methacrolein (META)	0.24	44	23	5.6	1.0	BDL	1.6	2.2	6.3	7.2
Butyraldehyde (BUTA)	1.4	36	16	3.1	1.1	1.1	1.1	4.5	3.5	6.2
Methyl Ethyl Ketone (MEK)	0.87	37	20	5.2	1.0	0.60	0.71	1.3	4.3	3.6
Benzaldehyde (BENA)	1.6	26	14	6.2	2.1	0.94	1.2	2.3	5.8	5.4
Valeraldehyde (VALA)	1.9	20	9.0	5.8	1.9	0.94	1.7	4.8	5.0	5.9
m-Tolualdehyde (m-TOLA)	0.13	8.7	2.0	0.20	0.55	0.09	0.01	0.33	0.29	0.73
Hexaldehyde (HEXA)	2.5	8.9	11	3.5	2.2	2.0	3.3	6.6	3.7	7.4
Total carbonyls	42	1474	750	166	54	28	35	87	126	179

a)   BDL: below detection limit
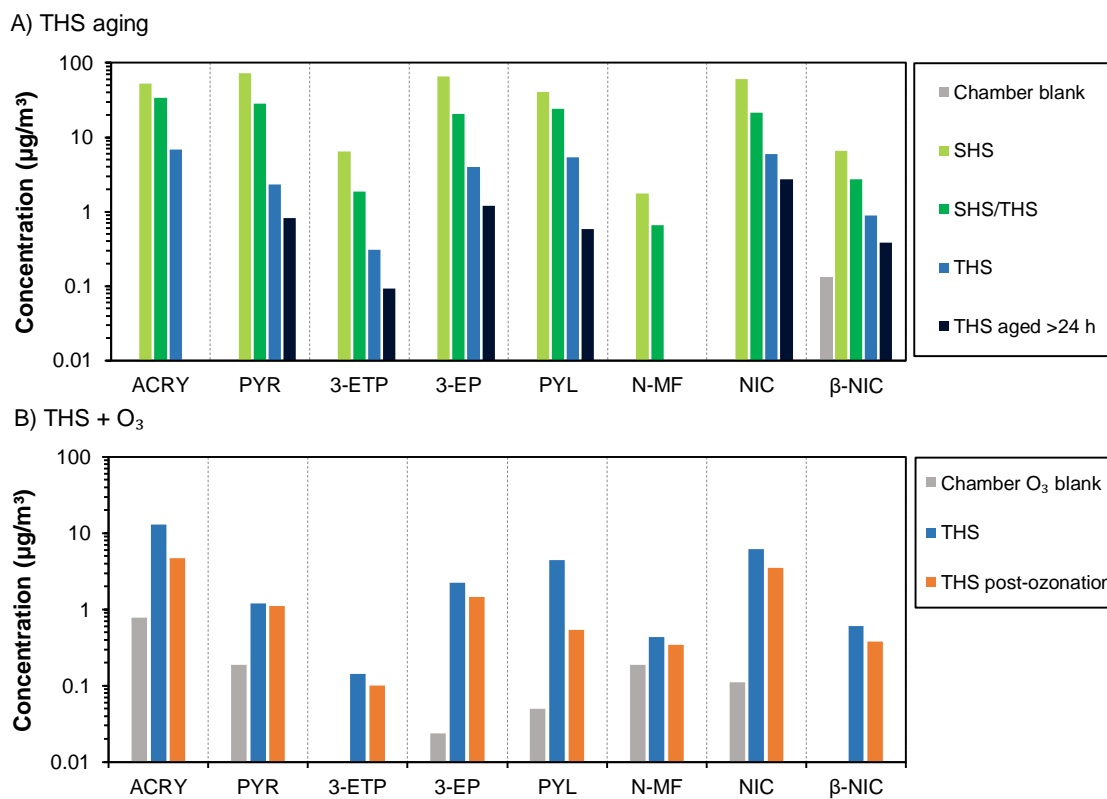
A) THS aging

B) THS + O₃

Figure S3: Nitrogenated VOCs in (A) THS aging and (B) THS+O₃ experiment.
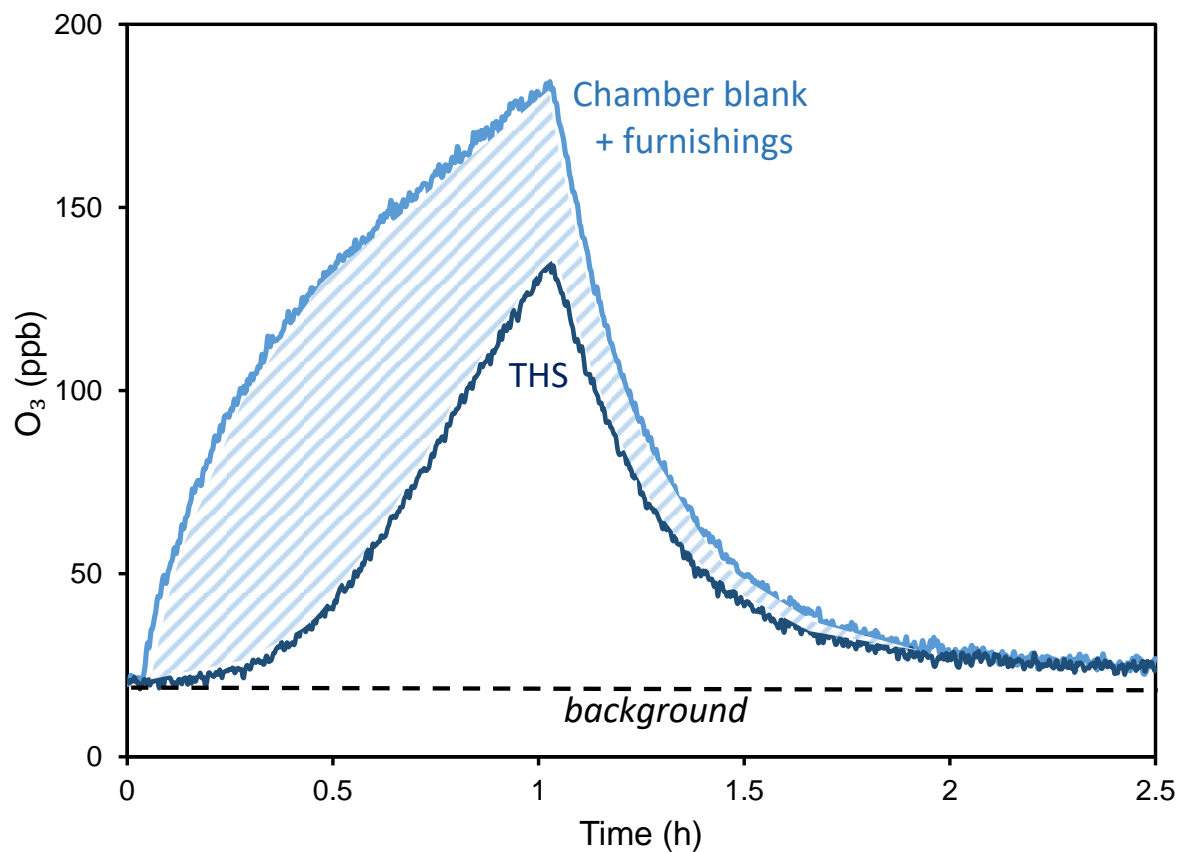
Figure S4: Ozone concentration profiles corresponding to ozonation of the chamber after installing furnishings (light blue) and 17.2 hours after smoking (THS, dark blue). The shaded area between those curves is proportional to the amount of ozone that reacted with THS.